SPCBIC 2021

25th – 28th October, Minna Nigeria

3RD SCHOOL OF PHYSICAL SCIENCES BIENNIAL INTERNATIONAL CONFERENCE
(SPSBIC 2021)

PROCEEDINGS

THEME:
THE ROLE OF SCIENCE AND TECHNOLOGY IN THE REALIZATION OF RESEARCH AND DEVELOPMENT IN THE ERA OF GLOBAL PANDEMIC

FEDERAL UNIVERSITY OF TECHNOLOGY MINNA, NIGER STATE, NIGERIA

A NOTE ON COMBUSTIBLE FOREST MATERIAL (CFM) OF WILDLAND FIRE SPREAD

Zhiri, A. B. [1*]; Olayiwola, R. O.[2] and Somma, S. A.[3]

[1,2,3]Department of Mathematics

Federal University of Technology, Minna, Nigeria.

[*1]a.zhiri@futminna.edu.ng

[2]olayiwola.rasaq@futminna.edu.ng

[3]sam.abu@futminna.edu.ng

Abstract:

In this paper, a mathematical model for combustible forest material of a wildland fire is presented. The equations describing the fractional components of forest fire were carefully studied. The reaction before a forest can burn or before fire can spread must involves fuel, heat and oxygen. The coupled dimensionless equations describing the phenomenon have been decoupled using perturbation method and solved analytically using eigen function expansion technique. The results obtained were graphically discussed and analysed. The study revealed that varying Radiation number and Peclet energy number enhances volume fractions of dry organic substance and moisture while they reduced volume fraction of coke.

Keywords& Phrases : Combustion, eigen function expansion, fire, fuel, ignition

1. Introduction

Fire is a natural disturbance that occurs in most terrestrial ecosystems around the world. It is also a tool that has been used by humans to manage a wide range of natural ecosystems worldwide. As such, it can produce a spectrum of effects on Combustible Forest Material (CFM) (dry organic substance, moisture and coke). CFM are part of the key factors to determine whether forest fire will escalate or not. Fons (1946) was the first to attempt to describe fire spread using a mathematical model. He focused his attention on the head of the fire where the fine fuels carry the fire and where there is ample oxygen to support combustion. He further, pointed out that sufficient heat is needed to bring the adjoining fuel to ignition temperature at the fire front. Therefore, he reasoned that fire spread in a fuel bed can be visualized as proceeding by a series of successive ignition and that its rate is controlled primarily by the ignition time and the distance between particles. Finney *et al.* (2013) reported that most studies on the effect of Fuel Moisture Content (FMC) have focused on dead fuel moisture (Md); thus, understanding on the mechanisms of fire spread in live vegetation is minimal.

Rossa *et al.* (2016) investigate live fuel complexes which are usually tall and have high fuel loads, so are difficult to reproduce in the laboratory. On the other hand, in field fires, live and dead fuels are usually combined in variable proportions and there is a lack of control over ambient parameters, which complicates the detection and isolation of FMC effects on fire be haviour. However, vegetation types dominated by live fuel (such as shrub lands) contribute

to a significant fraction of fire activity worldwide. Schaaf*et al.* (2007) examined that theoretical formulations of fire spread applied to shrub fuels or crown fires usually predict a strong spread ratedecrease with increased fuel moisture.

Perminov (2018) worked on mathematical modelling of wildland fires initiation and spread using a coupled atmosphere-forest fire setting, he stated that mathematical model gives an opportunity to describe the different conditions of the crown forest fires spread taking account different weather conditions, state of combustible forest materials, which allows applying the given model for prediction and preventing fires. It overestimates the rate of crown forest fire spread that depends on crown properties: bulk density, moisture content of forest fuel, wind velocity and the influence of boundary layer of atmosphere.

The purpose of this paper is to investigate the resultant effects of the dimensionless parameters as involved in the system in relation to CFM. We established an analytical solution using eigen function expansion technique.

2. Materials and Method

Model Formulations
Here we extend the work of (Perminov, 2018) in regards to wildfire spread model. We assume that the gas phase is made up of only oxygen, there is thermal equilibrium between the gas and solid phases, pressure and wind velocity of the forest canopy are constant, ash is neglected and the forest environment consist of five-phase porous medium which are dry organic substance (Matter), water in liquid state (Moisture), solid pyrolysis product (coke), ash and gas phase. Under these assumptions, the equations that describes wildland fire propagation are:

$$\left.\begin{aligned} &\rho_g\left(\frac{\partial C_{ox}}{\partial t}+v\frac{\partial C_{ox}}{\partial x}\right)=\frac{\partial}{\partial x}\left(\rho_g D_T\frac{\partial C_{ox}}{\partial x}\right)-\frac{\alpha}{C_{pg}\Delta h}\left(C_{ox}-C_{ox_\infty}\right)-\\ &\left(1-\alpha_c\right)k_1\rho_s\varphi_s C_{ox}e^{-\frac{E_1}{RT}}-k_2\rho_m T^{\frac{1}{2}}\varphi_m C_{ox}e^{\frac{-E_2}{RT}}-k_3 S_\sigma\rho_g\left(1+\frac{M_c}{M_1}C_{ox}\right)\varphi_c C_{ox}e^{\frac{-E_3}{RT}} \end{aligned}\right\} \quad (1)$$

$$\left.\begin{aligned} &\left(\phi\rho_g C_{pg}+\left(1-\phi\right)\sum_{i=1}^{s+m+c}\rho_i C_{pi}\varphi_i\right)\frac{\partial T}{\partial t}+\rho_g C_{pg}v\frac{\partial T}{\partial x}=\frac{\partial}{\partial x}\left(\lambda_T\frac{\partial T}{\partial x}\right)-\frac{\alpha}{\Delta h}\left(T-T_\infty\right)\\ &-4K_R\sigma T^4-k_2\rho_m q_2 T^{\frac{1}{2}}\varphi_m e^{\frac{-E_2}{RT}}+k_3 S_\sigma\rho_g q_3\varphi_c C_{ox}e^{\frac{-E_3}{RT}} \end{aligned}\right\} \quad (2)$$

$$\rho_s\frac{\partial\varphi_s}{\partial t}=-R_s,\ \rho_m\frac{\partial\varphi_m}{\partial t}=-R_m,\rho_c\frac{\partial\varphi_c}{\partial t}=-\alpha R_s-\frac{M_c}{M_1}R_c \quad (3)$$

$$\left.\begin{aligned} &\varphi_s\left(x,0\right)=\varphi_{so},\ \varphi_m\left(x,0\right)=\varphi_{mo},\ \varphi_c\left(x,0\right)=\varphi_{co},\ C_{ox}\left(x,0\right)=C_{ox_o},\ C_{ox}\left(0,t\right)=C_{ox_\infty}\\ &C_{ox}\left(\text{L},t\right)=C_{ox_\infty},\ T\left(x,0\right)=T_o,\ T\left(0,t\right)=T_\infty,\ T\left(\text{L},t\right)=T_\infty \end{aligned}\right\}$$
$$(4)$$

Such that;

$$
\left.
\begin{aligned}
R_s &= k_1 \varphi_s \rho_s \exp\left(-\frac{E_1}{RT}\right) \\[2mm]
R_m &= k_2 \varphi_m T^{\frac{1}{2}} \rho_m \exp\left(-\frac{E_2}{RT}\right) \\[2mm]
R_c &= k_3 S_\sigma \rho_g \varphi_c C_{ox} \exp\left(-\frac{E_3}{RT}\right)
\end{aligned}
\right\} \tag{5}
$$

where;

$(\varphi_s, \varphi_m, \varphi_c)$ define volume fractions of the multiphase reactive medium, that is φ_s corresponds to dry organic substance, φ_m is the moisture in liquid drop state combined with CFM, φ_c is coke(condensed pyrolysis product), C_{ox} is the concentration of oxygen, T is the temperature (in Kelvin), t is the time, x is a coordinate in the system of coordinates connected with the centre of an initial fire (distance), T_∞ is the unperturbed ambient temperature, $k_j, j = 1, 2, 3$ are the pre- exponential factors of chemical reactions, $E_j, j = 1, 2, 3$ are the activation energy of chemical reactions, C is the concentration, R is the universal gas constant, S_σ is the specific surface of the condensed product of pyrolysis (coke), v is the equilibrium wind velocity vector, U is the reference velocity, λ_T is the turbulent thermal conductivity, C_{ox_∞} is the unperturbed density of concentration of oxygen, $P_i, i = (s, m, c)$ is the i^{-th} phase density, that is ρ_s is the density of dry organic substance, ρ_m is the density of moisture, ρ_c is the density of coke, ρ_g is the density of gas phase (a mix of gases), Δh is the crown height, M_c is the molecular mass of carbon, M_1 is the mass of combustible forest material (CFM), C_{pg} is the thermal capacity of a gas phase, $q_j, j = 2, 3$ defines heat effects of processes of evaporation of burning, D_T is the diffusion coefficient, α is the coefficient of heat exchange between the atmosphere and a forest canopy, R_s, R_m, R_c are mass rates of reactions of dry CFM pyrolysis (chemical decomposition of substance by heating with allocation of combustible gases), of moisture evaporation from CFM (drying), coke burning, α_c is the coke number of combustible forest material (CFM), σ is the Stefan-BoltzMann constant, K_R is the integrated absorptance, $C_{p_i}, i = (s, m, c)$ is the i^{-th} phase of thermal capacity, s is the dry organic substance, m is the moisture, c is the coke, ox is the oxygen (O_2).

Our mathematical modelabove consists of equations (1)—(3) such that (1) and (2) corresponds to mass concentration of oxygen and energy balance respectively, (3) describes the volume fractions of the multiphase reactive medium (dry organic substance, moisture and coke respectively), (4) is the initial and boundary conditions and (5) is the mass rate of chemical reaction that describes the speed of CFM.

3. Method of Solution
3.1 Non-dimensionalisation
We make the variables in equation (1) – (4) dimensionless by introducing the following dimensionless variables:

$$x' = \frac{x}{L}, \ t' = \frac{Ut}{L}, \ v' = \frac{v}{U}, \ \psi_1 = \frac{\varphi_s}{\varphi_{so}}, \ \psi_2 = \frac{\varphi_m}{\varphi_{mo}}, \ \psi_3 = \frac{\varphi_c}{\varphi_{co}}, \ \phi = \frac{C_{ox} - C_{ox_\infty}}{C_{ox_o} - C_{ox_\infty}}$$

$$\in = \frac{RT_0}{E}, \ \theta = \frac{E(T - T_o)}{RT_o^2}, \ f = \frac{E_1}{E_3}, \ r = \frac{E_2}{E_3} \tag{6}$$

Then equation (1)—(4) (after dropping prime) becomes;

$$\frac{\partial \phi}{\partial t} + v \frac{\partial \phi}{\partial x} = \frac{\partial}{\partial x} \left(D_1 \frac{\partial \phi}{\partial x} \right) - \beta_1 \phi - \beta_2 \psi_1 (\phi + q) e^{\frac{f\theta}{1+\in\theta}}$$

$$- \beta_3 (1 + \in \theta)^{\frac{1}{2}} \psi_2 (\phi + q) e^{\frac{r\theta}{1+\in\theta}} - \beta_4 \psi_3 (\phi + p)(\phi + q) e^{\frac{\theta}{1+\in\theta}} \tag{7}$$

$$\frac{\partial \theta}{\partial t} + v \frac{\partial \theta}{\partial x} = \frac{\partial}{\partial x} \left(\lambda_1 \frac{\partial \theta}{\partial x} \right) - \alpha_1 (\theta + \gamma_1) - R_a (1 + 4 \in \theta) - \delta \psi_2 (1 + \in \theta)^{\frac{1}{2}} e^{\frac{r\theta}{1+\in\theta}}$$

$$+ \delta_1 \psi_3 (\phi + q) e^{\frac{\theta}{1+\in\theta}} \tag{8}$$

$$\frac{\partial \psi_1}{\partial t} = -a \psi_1 e^{\frac{f\theta}{1+\in\theta}}; \ \frac{\partial \psi_2}{\partial t} = -b \psi_2 (1 + \in \theta)^{\frac{1}{2}} e^{\frac{r\theta}{1+\in\theta}};$$

$$\frac{\partial \psi_3}{\partial t} = \beta \psi_1 e^{\frac{f\theta}{1+\in\theta}} - \gamma (\phi + q) \psi_3 e^{\frac{\theta}{1+\in\theta}} \tag{9}$$

$$\psi_1(x,0) = 1, \ \psi_2(x,0) = 1, \ \psi_3(x,0) = 1$$

$$\phi(x,0) = 1, \quad \phi(0,t) = 0, \quad \phi(1,t) = 0 \tag{10}$$

$$\theta(x,0) = 0, \quad \theta(0,t) = \sigma_1, \quad \theta(1,t) = \sigma_1$$

where;

$$a = \frac{k_1 L e^{\frac{-fE_1}{RT_o}}}{U}, \quad b = \frac{k_2 T_o^{\frac{1}{2}} L e^{\frac{-rE_3}{RT_0}}}{U}, \quad \beta = \frac{\alpha_c k_1 \rho_s \varphi_{so} L e^{\frac{-fE_3}{RT_o}}}{U \rho_c \varphi_{co}}, \quad \gamma = \frac{M_c k_3 S_\sigma \rho_g L}{M_1 U \rho_c} \left(C_{ox_o} - C_{ox_\infty} \right) e^{\frac{-E_3}{RT_o}},$$

$$q = \frac{C_{ox_\infty}}{C_{ox_o} - C_{ox_\infty}}, \quad D_1 = \frac{D_T}{LU} = \frac{1}{P_{em}}, \quad \beta_1 = \frac{\alpha L}{C_{pg} \Delta h U}, \quad \beta_2 = \frac{(1-\alpha_c) k_1 \rho_s \varphi_{so} L}{\rho_g U} e^{\frac{-fE_3}{RT_o}},$$

$$\beta_3 = \frac{k_2 \rho_m T_o^{\frac{1}{2}} \varphi_{mo} L e^{\frac{-rE_3}{RT_o}}}{\rho_g U}, \quad \beta_4 = \frac{k_3 S_\sigma \rho_g \frac{M_c}{M_1} \left[C_{ox_o} - C_{ox_\infty} \right] L \varphi_{co} e^{\frac{-E_3}{RT_o}}}{\rho_g U}, \quad p = \frac{\frac{M_1}{M_c} + C_{ox_\infty}}{C_{ox_o} - C_{ox_\infty}},$$

$$\lambda_1 = \frac{\lambda_T}{L \rho_g C_{pg} U} = \frac{1}{P_e}, \quad \alpha_1 = \frac{\alpha L}{\rho_g C_{pg} U}, \quad R_a = \frac{4 K_R \sigma L T_o^3}{\rho_g C_{pg} \in U}, \quad \delta = \frac{k_2 \rho_m q_2 T_o^{\frac{1}{2}} L \varphi_{mo} e^{\frac{-rE_3}{RT_o}}}{\rho_g C_{pg} \in T_o U},$$

$$\delta_1 = \frac{k_3 S_\sigma \rho_g q_3 \varphi_{co} L \left(C_{ox_o} - C_{ox_\infty} \right)}{\rho_g C_{pg} \in T_o U} e^{\frac{-E_3}{RT_o}}, \quad \gamma_1 = \frac{T_o - T_\infty}{\in T_o}, \quad \sigma_1 = \frac{T_\infty - T_o}{\in T_o}$$

(11)

3.2 Approximate Analytical Solution

After Applying perturbation method to decouple equations (7)—(10), we then use direct integration and eigenfunction expansion technique, to obtain the approximate analytical solution of equations (7)—(10) as follows:

$$
\phi(x,t) = \sum_{n=1}^{\infty} A e^{-c_1 t} \sin n\pi x + v \left(\sum_{n=1}^{\infty} \left[\begin{array}{l} -2A_{49}\sum_{n=1}^{\infty} At e^{-c_1 t} - 2A_{50}\sum_{n=1}^{\infty}\left[\dfrac{A_1}{c_1} + A_{53}e^{-c_2 t} - A_{54}e^{-c_1 t} \right] \\[2mm] -A_{56}\left[1 - e^{-c_1 t}\right] - 2A_{51}\sum_{n=1}^{\infty}\sum_{n=1}^{\infty} A_{52}\left[\begin{array}{l} AA_1 te^{-c_1 t} - A_{55}e^{-(c_1+c_2)t} \\ + A_{55}e^{-c_1 t} \end{array}\right] \\[2mm] -2A_{42}\sum_{n=1}^{\infty}\sum_{n=1}^{\infty} A_{52}\left[\begin{array}{l} \dfrac{A_1^2}{c_1} + A_{57}e^{-c_2 t} + A_{58}e^{-2c_2 t} - \dfrac{A_1^2}{c_1}e^{-c_1 t} \\ - A_{57}e^{-c_1 t} - A_{58}e^{-c_1 t} \end{array}\right] \\[2mm] -2A_{43}\sum_{n=1}^{\infty}\sum_{n=1}^{\infty}\sum_{n=1}^{\infty}\left[\begin{array}{l} AA_1^2 te^{-c_1 t} - A_{59}e^{-(c_1+c_2)t} \\ - A_{59}e^{-(c_1+c_2)t} - A_{60}e^{-(c_1+2c_2)t} \\ + A_{59}e^{-c_1 t} + A_{59}e^{-c_1 t} + A_{60}e^{-c_1 t} \end{array}\right] \\[2mm] + 2A_{44}\sum_{n=1}^{3}\sum_{n=1}^{3} A_{61}\left[1 - e^{-c_1 t}\right] - 2A_{45}\sum_{n=1}^{\infty}\sum_{n=1}^{\infty} A_{52}\left[\begin{array}{l} AA_1 te^{-c_1 t} \\ -A_{55}e^{-(c_1+c_2)t} \\ + A_{55}e^{-c_1 t} \end{array}\right] \\[2mm] + 2A_{46}\sum_{n=1}^{\infty}\sum_{n=1}^{\infty}\sum_{n=1}^{\infty}\left[A_{62}e^{-2c_1 t} + A_{63}e^{-(2c_1+c_2)t} - A_{62}e^{-c_1 t} - A_{63}e^{-c_1 t}\right] \end{array}\right] \right) \sin n\pi x \tag{12}
$$

$$
\theta(x,t) = \left(\sigma_1 + \sum_{n=1}^{\infty}\left(A_1 + (b_n - A_1)e^{-c_2 t}\right)\sin n\pi x \right) +
$$
$$
v\left(\sum_{n=1}^{\infty}\left[\begin{array}{l} -2\dfrac{A_{72}}{c_2}\left[1 - e^{-c_2 t}\right] - 2A_{73}\sum_{n=1}^{\infty}\left[\dfrac{A_1}{c_2} + (b_n - A_1)te^{-c_2 t} - \dfrac{A_1}{c_2}e^{-c_2 t}\right] \\[2mm] -2A_{68}\sum_{n=1}^{\infty}\sum_{n=1}^{\infty} A_{52}\left[\begin{array}{l} \left[1 - e^{-c_2 t}\right]\dfrac{A_1^2}{c_2} + 2A_1(b_n - A_1)te^{-c_2 t} \\ + \left[e^{-c_2 t} - 1\right]\dfrac{(b_n - A_1)^2}{c_2} \end{array}\right] \\[2mm] + 2A_{69}\sum_{n=1}^{\infty}\dfrac{A}{(c_2 - c_1)}\left[e^{-c_1 t} - e^{-c_2 t}\right] + 2A_{70}\sum_{n=1}^{\infty}\sum_{n=1}^{\infty} A_{52}\left[\begin{array}{l} \dfrac{AA_1}{(c_2-c_1)}e^{-c_1 t} - \dfrac{A(b_n - A_1)}{c_1}e^{-(c_2+c_1)t} \\ - \dfrac{AA_1}{(c_2-c_1)}e^{-c_2 t} + \dfrac{A(b_n - A_1)}{c_1}e^{-c_2 t} \end{array}\right] \end{array}\right] \sin n\pi x \right) \tag{13}
$$

$$
\psi_1(x,t) = 1 + v\left(-A_3\sum_{n=1}^{\infty} A_2 \sin n\pi x - a_6\left(t + \left(\begin{array}{l} f(e-2). \\ \left(\sigma_1 t + \sum_{n=1}^{\infty}\left(A_1 t - A_2 e^{-c_2 t}\right)\sin n\pi x\right) \end{array}\right)\right)\right) \tag{14}
$$

$$\psi_2(x,t) = 1 + v\left(\begin{array}{l} -a_7\left(\begin{array}{l} \left(t + r(e-2)\right)\left(\sigma_1 t + \sum_{n=1}^{\infty}\left(A_1 t - A_2 e^{-c_2 t}\right)\sin n\pi x\right) + \\[2mm] \dfrac{1}{2}\in\left(\sigma_1 t + \sum_{n=1}^{\infty}\left(A_1 t - A_2 e^{-c_2 t}\right)\sin n\pi x\right) + \\[2mm] \dfrac{1}{2}\in\left(r(e-2)\right)\left(\begin{array}{l}\sigma_1^2 t + 2\sigma_1\left(\sum_{n=1}^{\infty}\left(A_1 t - A_2 e^{-c_2 t}\right)\sin n\pi x\right) \\[2mm] +\sum_{n=1}^{\infty}\sum_{n=1}^{\infty}\left(\begin{array}{l} A_1^2 t - \dfrac{2A_1}{c_2}\left(b_n - A_1\right)e^{-c_2 t} \\[2mm] -\dfrac{\left(b_n - A_1\right)^2}{2c_2}e^{-2c_2 t}\end{array}\right)\sin^2 n\pi x\end{array}\right) \end{array}\right) \\[10mm] -a_7\left(A_7 + \sum_{n=1}^{\infty}B_1 \sin n\pi x\right)\sum_{n=1}^{\infty}A_2 \sin n\pi x \end{array}\right) \qquad (15)$$

$$\psi_3(x,t) = 1 + v\left(\begin{array}{l} a_9\left(A_8 t + A_9\sum_{n=1}^{\infty}\left(A_1 t - A_2 e^{-c_2 t}\right)\sin n\pi x\right) \\[3mm] +a_8\left(\begin{array}{l} A_{10}\sum_{n=1}^{\infty}\dfrac{A}{c_1}e^{-c_1 t}\sin n\pi x + A_{11}\sum_{n=1}^{\infty}\sum_{n=1}^{\infty}\left(B_2 e^{-c_1 t} + B_3 e^{-(c_1+c_2)t}\right)\sin^2 n\pi x \\[3mm] -A_{12}t - A_{13}\sum_{n=1}^{\infty}\left(A_1 t - A_2 e^{-c_2 t}\right)\sin n\pi x \end{array}\right) \\[6mm] +a_9 A_9\sum_{n=1}^{\infty}A_2 \sin n\pi x - a_8\left(\begin{array}{l} A_{10}\sum_{n=1}^{\infty}\dfrac{A}{c_1}\sin n\pi x + A_{11}\sum_{n=1}^{\infty}\sum_{n=1}^{\infty}\left(B_4\right)\sin^2 n\pi x \\[3mm] +A_{13}\sum_{n=1}^{\infty}A_2 \sin n\pi x \end{array}\right) \end{array}\right) \qquad (16)$$

where;

$$c_1 = \left(\beta_1 + D_1 \left(n\pi\right)^2\right), \ A = \frac{2\left[1-\left(-1\right)^n\right]}{n\pi}, \ b_1 = \left(4R_a \in +\alpha_1\right), \ b_2 = \left(\sigma_1\left(4R_a \in +\alpha_1\right)+\left(R_a+\alpha_1\gamma_1\right)\right),$$

$$c_2 = \left(b_1 + \lambda_1\left(n\pi\right)^2\right), \ A_1 = \frac{2b_2\left[\left(-1\right)^n-1\right]}{n\pi c_2}, \ A_2 = \left(\frac{b_n-A_1}{c_2}\right), \ A_3 = a_6 f\left(e-2\right), \ A_4 = r\left(e-2\right),$$

$$A_5 = \frac{1}{2}\in, \ A_6 = \in\left(r\left(e-2\right)\right)\sigma_1, \ B = \frac{b_n-A_1}{2}, \ B_1 = \left(2A_1+B\right), \ A_7 = \left(A_4+A_5+A_6\right), \ b_n = \frac{2\sigma_1}{n\pi}\left[\left(-1\right)^n-1\right]$$

$$A_8 = \left(1+f\left(e-2\right)\sigma_1\right), \ A_9 = f\left(e-2\right), \ A_{10} = \left(1+\left(e-2\right)\sigma_1\right), \ A_{11} = \left(e-2\right), \ B_2 = \frac{AA_1}{c_1},$$

$$B_3 = \frac{A\left(b_n-A_1\right)_1}{c_1+c_2}, \ A_{12} = \left(1+\left(e-2\right)\sigma_1\right)q, \ A_{13} = \left(e-2\right)q, \ B_4 = \left(B_2+B_3\right), \ A_{14} = \left(1+f\left(e-2\right)\sigma_1\right)q,$$

$$A_{15} = f\left(e-2\right)q, \ A_{16} = \left(1+r\left(e-2\right)\sigma_1\right), \ A_{17} = r\left(e-2\right), \ A_{18} = \left(1+r\left(e-2\right)\sigma_1\right)q, \ A_{19} = r\left(e-2\right)q,$$

$$A_{20} = \frac{1}{2}\in\left(\left(1+r\left(e-2\right)\sigma_1\right)\sigma_1\right), \ A_{21} = \frac{1}{2}\in r\left(e-2\right)\sigma_1, \ A_{22} = \frac{1}{2}\in\left(\left(1+r\left(e-2\right)\sigma_1\right)\sigma_1 q\right),$$

$$A_{23} = \frac{1}{2}\in r\left(e-2\right)\sigma_1 q, \ A_{24} = \frac{1}{2}\in\left(1+r\left(e-2\right)\sigma_1\right), \ A_{25} = \frac{1}{2}\in r\left(e-2\right), \ A_{26} = \frac{1}{2}\in\left(1+r\left(e-2\right)\sigma_1\right)q,$$

$$A_{27} = \frac{1}{2}\in r\left(e-2\right)q, \ A_{28} = \left(p+q\right)\left(1+\left(e-2\right)\sigma_1\right), \ A_{29} = \left(p+q\right)\left(e-2\right), \ A_{30} = \left(pq\right)\left(1+\left(e-2\right)\sigma_1\right),$$

$$A_{31} = \left(pq\right)\left(e-2\right), \ A_{32} = \left(a_1 A_{14}+a_2 A_{18}+a_2 A_{22}+a_3 A_{30}\right), \ A_{33} = \left(a_1 A_{16}+a_2 A_{20}\right), \ A_{34} = \left(a_2 A_{19}+a_2 A_{23}+a_2 A_{26}\right),$$

$$A_{35} = \left(a_2 A_{17}+a_2 A_{21}+a_2 A_{22}+a_2 A_{24}\right), \ A_{36} = \frac{1}{2}a_1 A_8, \ A_{37} = \frac{1}{2}a_1 A_{15}, \ A_{38} = \frac{2}{3}a_1 A_9, \ A_{39} = \frac{1}{2}A_{33}, \ A_{40} = \frac{1}{2}A_{34},$$

$$A_{41} = \frac{2}{3}A_{35}, \ A_{42} = \frac{2}{3}a_2 A_{27}, \ A_{43} = \frac{3}{8}a_2 A_{25}, \ A_{44} = \frac{2}{3}a_3 A_{10}, \ A_{45} = \frac{2}{3}a_3 A_{29}, \ A_{46} = \frac{3}{8}a_3 A_{11}, \ A_{47} = \frac{1}{2}a_3 A_{38},$$

$$A_{48} = \frac{1}{2}a_3 A_{31}, \ A_{49} = \left(A_{36}+A_{39}+A_{47}\right), \ A_{50} = \left(A_{37}+A_{40}+A_{48}\right), \ A_{51} = \left(A_{38}+A_{41}\right), \ A_{52} = \left[\frac{1-\left(-1\right)^n}{n\pi}\right],$$

$$A_{53} = \frac{b_n-A_1}{c_1-c_2}, \ A_{54} = \frac{A_1\left(c_1-c_2\right)+c_1\left(b_n-A_1\right)}{c_1\left(c_1-c_2\right)}, \ A_{55} = \frac{A\left(b_n-A_1\right)}{c_2}, \ A_{56} = 2\frac{A_{32}A_{52}}{c_1}, \ A_{57} = \frac{2A_1\left(b_n-A_1\right)}{c_1-c_2},$$

$$A_{58} = \frac{\left(b_n-A_1\right)^2}{\left(c_1-2c_2\right)}, \ A_{59} = \frac{AA_1\left(b_n-A_1\right)}{c_2}, \ A_{60} = \frac{A\left(b_n-A_1\right)^2}{2c_2}, \ A_{61} = \frac{A_{52}A^2}{c_1}, \ A_{62} = \frac{A^2 A_1}{c_1}, \ A_{63} = \frac{A^2\left(b_n-A_1\right)}{\left(c_1+c_2\right)},$$

$$A_{64} = \left(a_4 A_{16}+a_4 A_{20}-a_5 A_{12}\right), \ A_{65} = \frac{a_4 A_{17}}{2}, \ A_{66} = \frac{a_4 A_{21}}{2}, \ A_{67} = \frac{a_4 A_{24}}{2}, \ A_{68} = \frac{2a_4 A_{25}}{3}, \ A_{69} = \frac{a_5 A_{10}}{2},$$

$$A_{70} = \frac{2a_5 A_{11}}{3}, \ A_{71} = \frac{a_5 A_{13}}{2}, \ A_{72} = \left(A_{64}A_{52}\right), \ A_{73} = \left(A_{65}+A_{66}+A_{67}-A_{71}\right)$$

The computation were done using computer symbolic algebraic package MAPLE to generate the graphs.

4. Results and Discussion

We solve the systems of partial differential equations describing the fractional components of forest fire. We decoupled the equations using perturbation method. The effectof Radiation number (R_a) and Pecletenergy number (P_e) on Volume fractions of dry organic substance $\psi_1(x,t)$, moisture $\psi_2(x,t)$ and coke $\psi_3(x,t)$ were vividly discussed and analysed. Analytical solution given by equations (12)—(16), is computed using computer symbolic algebraic package MAPLE 17 to generate the graphs. The numerical results obtained from the method are then shown in Figures1, 2, 3, 4, 5 and 6.

Figure 1adisplays the graph of volume fraction of dry organic substance $\psi_1(x,t)$ against time t for different values of Radiation number (R_a). It is observed that the volume fraction of dry organic substance decreases with time and increases as the Radiation number increases.

Figure 1bdepicts the graph of volume fraction of dry organic substance $\psi_1(x,t)$ against distance x for different values of Radiation number (R_a). It is observed that the volume fraction of dry organic substance increases but later decreases along the distance and maximum volume fraction of dry organic substance increases as the Radiation number increases.

Figure 2adepicts the graph of volume fraction of moisture $\psi_2(x,t)$ against time t for different values of Radiation number (R_a). It is observed that the volume fraction of moisture decreases with time and increases as the Radiation number increases.

Figure 2b displays the graph of volume fraction of moisture $\psi_2(x,t)$ against distance x for different values of Radiation number (R_a). It is observed that the volume fraction of moisture increases but later decreases along the distance and maximum volume fraction of moisture increases as the Radiation number increases.

Figure 3a displays the graph of volume fraction of coke $\psi_3(x,t)$ against time t for different values of Radiation number (R_a). It is observed that the of volume fraction of coke increases with time and decreases as the Radiation number increases.

Figure 3b depicts the graph of volume fraction of moisture $\psi_2(x,t)$ against distance x for different values of Radiation number (R_a). It is observed that the volume fraction of coke

decreases but later increases along the distance and minimum volume fraction of coke decreases as the Radiation number increases.

Figure 4a depicts the graph of volume fraction of dry organic substance $\psi_1(x,t)$ against time t for different values of Peclet energy number (P_e). It is observed that the volume fraction of dry organic substance decreases with time and increases as Peclet energy number increases.

Figure 4b displays the graph of volume fraction of dry organic substance $\psi_1(x,t)$ against distance x for different values of Peclet energy number (P_e). It is observed that the volume fraction of dry organic substance increases but later decreases along the distance and maximum volume fraction of dry organic substance increases as the Peclet energy number increases.

Figure 5a depicts the graph of volume fraction of moisture $\psi_2(x,t)$ against time t for different values of Peclet energy number (P_e). It is observed that the of volume fraction of moisture decreases with time and increases as the Peclet energy number increases.

Figure 5b depicts the graph of volume fraction of moisture $\psi_2(x,t)$ against distance x for different values of Peclet energy number (P_e). It is observed that the volume fraction of moisture increases but later decreases along the distance and maximum volume fraction of moisture increases as the of Peclet energy number increases.

Figure 6a displays the graph of volume fraction of coke $\psi_3(x,t)$ against time t for different values of Peclet energy number (P_e). It is observed that the of volume fraction of coke increases with time and decreases as the Peclet energy number increases.

Figure 6b depicts the graph of volume fraction of coke $\psi_3(x,t)$ against distance x for different values of Peclet energy number (P_e). It is observed that the volume fraction of coke decreases but later increases along the distance and decreases as Peclet energy number increases.
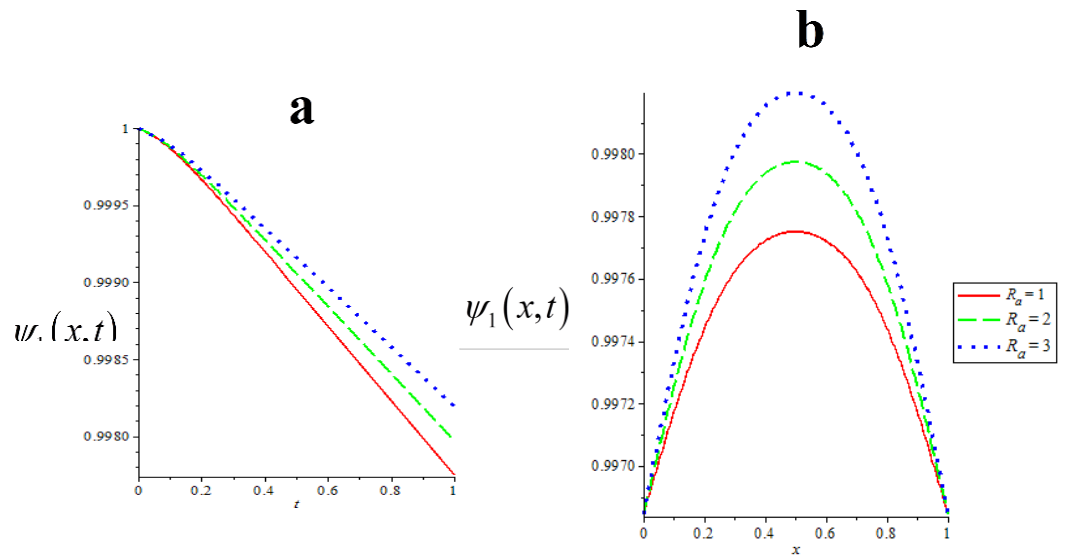
Figure 1: Effect of Radiation number (R_a) on volume fraction of dry organic substance.
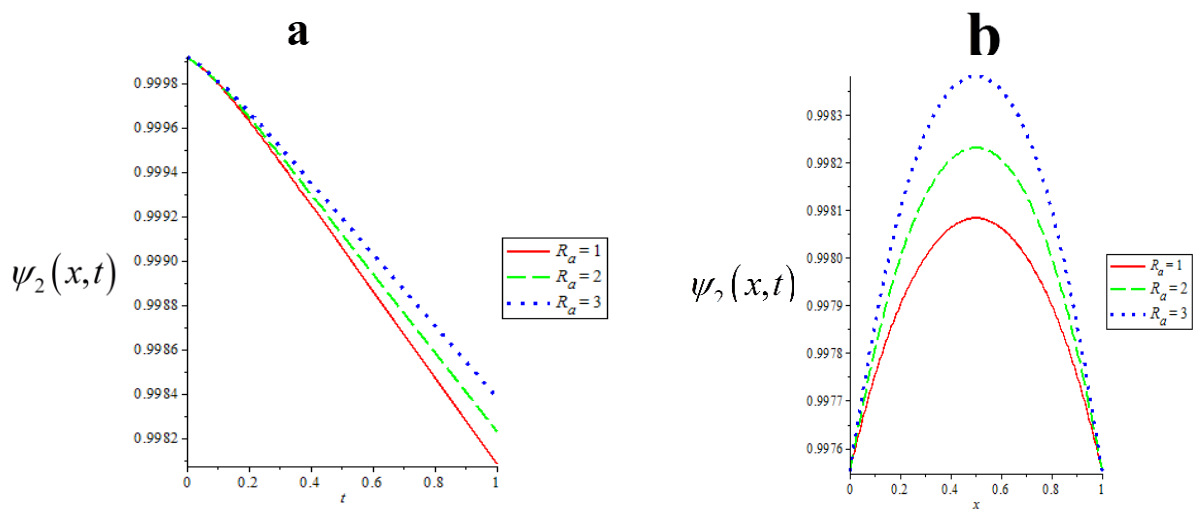

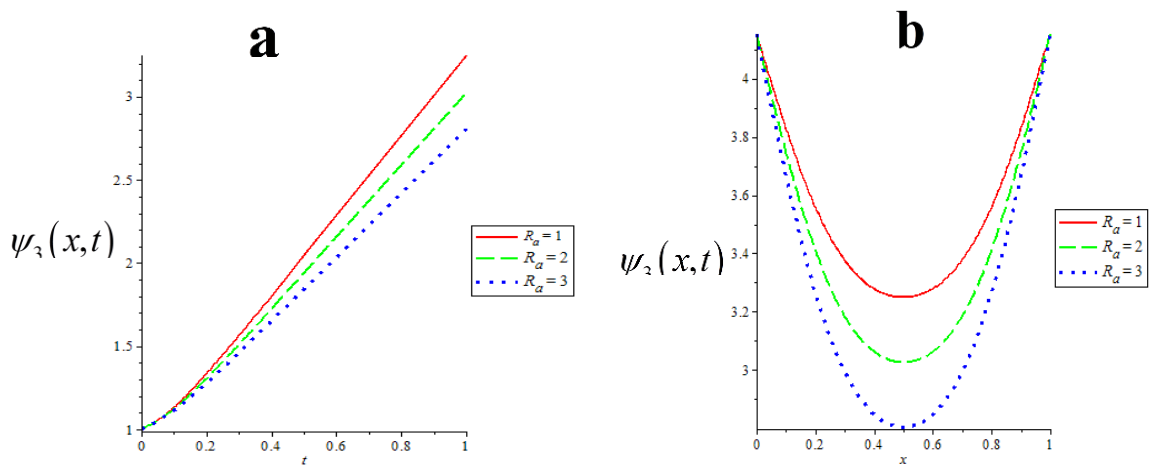Figure 2: Effect of Radiation number (R_a) on volume fraction of moisture.

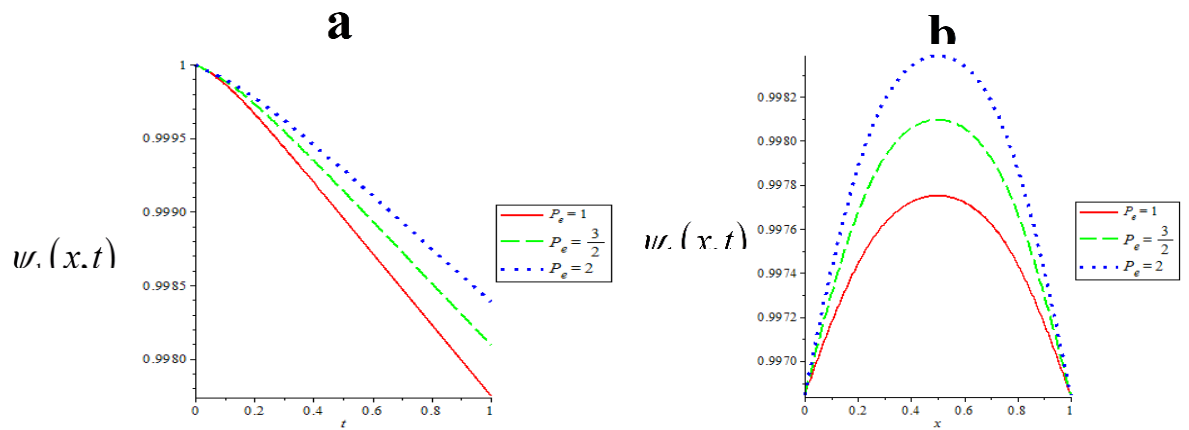Figure 3: Effect of Radiation number $\left(R_a\right)$ on volume fraction of coke.

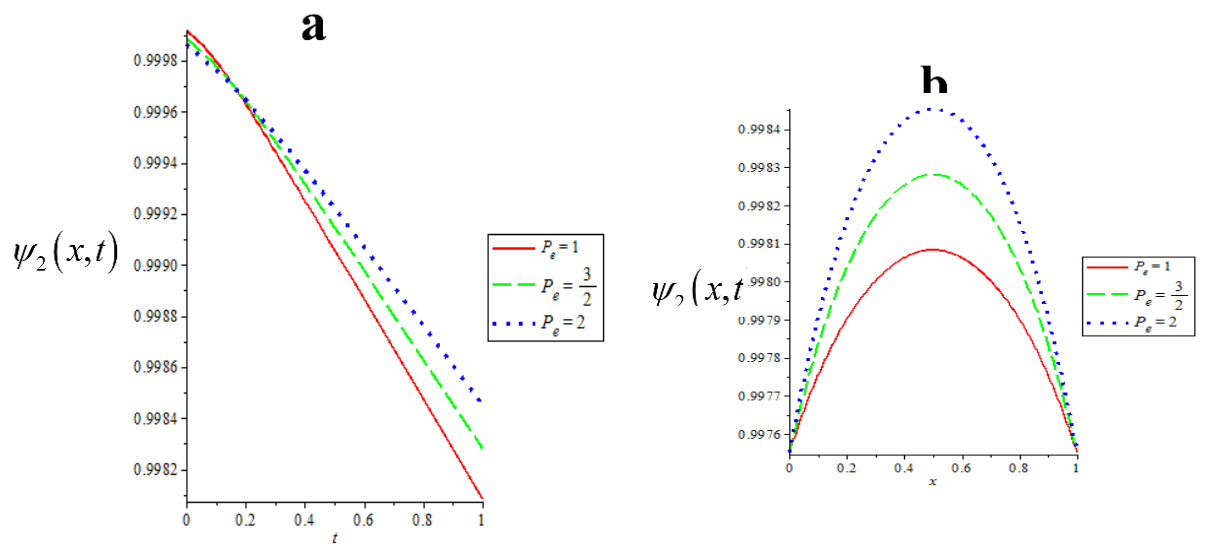Figure 4: Effect of Peclet energy number $\left(P_e\right)$ on volume fraction of dry organic substance.

Figure 5: Effect of Peclet energy number $\left(P_e\right)$ on volume fraction of moisture.
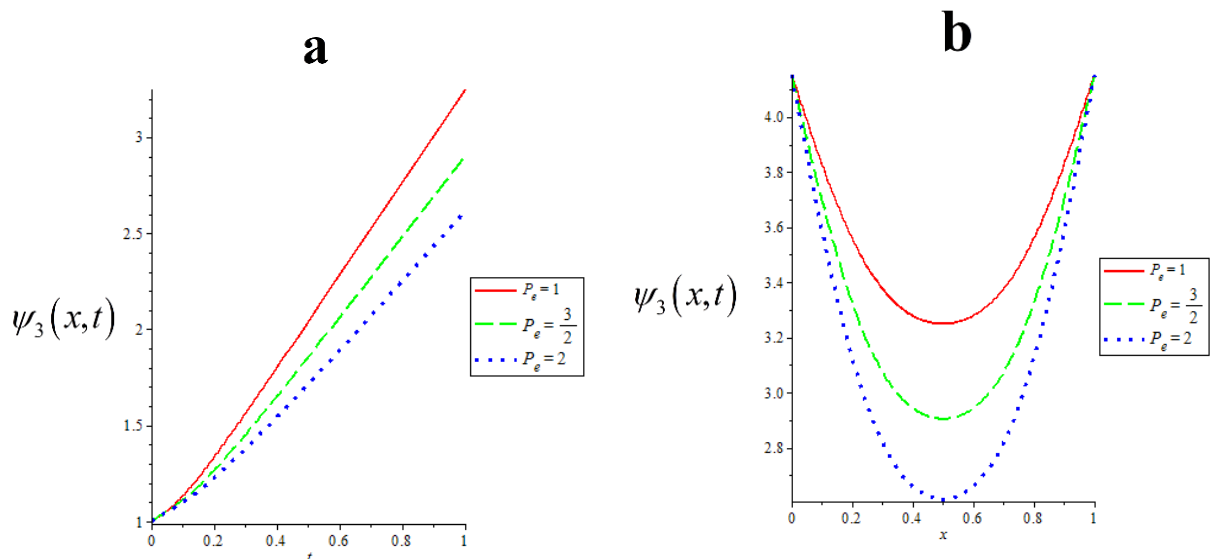
a **b**

Figure 6: Effect of Peclet energy number $\left(P_e\right)$ on volume fraction of coke

5. Conclusion

From the results of our studies we conclude that radiation number and peclect energy number enhance the volume fractions of dry organic substance and moisture and decrease volume fraction of coke. These occur as a result of varying the dimensionless parameters as demonstrated in Figures 1, 2, 3, 4, 5, and 6 respectively. The inference drawn from this study is that an increase in Radiation number and Peclet energy number reduces the burning rate of dry organic substance and dehydration of moisture. With continuous removal of heat from a burning scene, the CFM are better preserved. Based on this knowledge, the fire fighters or combaters are better equipped to manage CFM.

References

Finney, M. A., Cohen, J. D., McAllister, S. S. & Jolly, W. M. (2013) On the need for a theory of wildland fire spread. *International Journal of Wildland Fire* **22**(1), 25–36. doi:10.1071/WF11117

Fons, W. (1946). Analysis of fire spread in light forest fuels. *J. Agr. Res.* 72(3):93-121, illus.

Perminov, V. A. (2018). Mathematical modelling of wildland fires initiation and spread using a coupled atmospheric-forest fire setting, *The Italian Association of Chemical Engineering, 70, 1747-1752* doi: 10.3303/CET1870292 ISBN978-88-95608-67-9; ISSN 2283-9216

Rossa, C. G., Veloso, R. &Fernandes, P. M. (2016). A laboratory-based quantification of the ffect of live fuel moisture content on fire spread rate. *International Journal of Wildland Fire* **25**(5), 569–573. doi:10.1071/WF15114.

Schaaf, M. D., Sandberg, D. V., Schreuder, M. D. &Riccardi, C. L. (2007). A conceptual framework for ranking crown fire potential in wildland fuelbeds. *Canadian Journal of Forest Research* **37**, 2464–2478. doi:10.1139/X07-102.